Journal Name

Dynamic Article Links ►

Cite this: DOI: 10.1039/c0xx00000x

www.rsc.org/xxxxxx

ARTICLE TYPE

Electrochemical reduction of CO_2 in organic solvents catalyzed by MoO_2

Yeonji Oh, Heron Vrubel, Sébastien Guidoux, and Xile Hu*

Received (in XXX, XXX) Xth XXXXXXXXX 20XX, Accepted Xth XXXXXXXXX 20XX
DOI: 10.1039/b000000x

MoO_2 microparticles are an active catalyst for the electrochemical reduction of CO_2 in organic solvents such as acetonitrile and dimethylformamide. The catalytic activity and product selectivity depend on temperature and water content of the solvent.

CO_2 is a potent greenhouse gas and its dramatic increase in concentration in the earth's atmosphere due to the combustion of fossil fuels is a main contributor to the current climate change. On the other hand, CO_2 can be considered as an abundant and inexpensive carbon feedstock, especially if carbon sequestration is required for future fossil fuel-based power stations.[1] Electrochemical reduction of CO_2 to form useful chemicals or fuels is a potentially efficient method of CO_2 utilization and recycling. However, the kinetic inertness of CO_2 and the possibility of multiple products necessitate selective and energy-efficient catalysts for CO_2 reduction.[2-4] A large number of metal electrodes have been studied for CO_2 reduction in both aqueous and organic solutions.[2, 5, 6] Among those, coinage metals Cu,[7-11] Au,[12] and Ag[13] draw much recent attention. In addition, Bi is shown as a selective catalyst for CO_2 reduction in acetonitrile (MeCN).[14] Reports of metal oxides as catalysts for CO_2 reduction are, however, scarce. Kanan and co-workers reported that tin oxide significantly enhanced the CO_2 reduction activity of tin electrode, suggesting that metal oxides are promising candidates for CO_2 reduction.[15] Our interest in Mo-based electrocatalysts[16-18] led us to study the activity of MoO_2 for CO_2 reduction. We found that MoO_2 indeed catalyzed CO_2 reduction in organic solvents such as MeCN and dimethylformamide (DMF). Herein we describe the activity and product selectivity of this new catalytic system.

The MoO_2 particles used in this study have an average size of 30 μm (Figure S1, ESI). According to powder X-ray diffraction (XRD), monoclinic MoO_2 is the only crystalline phase present in the particles (Figure S2, ESI). Pb was chosen as the supporting substrate because of its high conductivity and softness which leads to a good binding of MoO_2 particles upon application of pressure. As shown below, under the conditions of our investigations, the background reduction of CO_2 by Pb is negligible, which makes Pb a suitable substrate. On the contrary, conventional substrates such as glassy carbon and FTO do not bind MoO_2 strongly so they cannot be used. The electrochemical measurements were conducted in a three-electrode cell in MeCN containing 0.1 M tetrabutylammonium hexafluorophosphate ($TBAPF_6$) as electrolyte at room temperature (RT) and -20 °C.

MeCN is a commonly used organic solvent for CO_2 electroreduction; the solubility of CO_2 in MeCN is eight-fold higher than in water.[19] A Pb pellet with 20 wt% MoO_2 was used as the working electrode. At RT, a significant catalytic current for CO_2 reduction was observed at about -2.0 V vs. the ferrocene/ferrocenium (Fe/Fc^+) couple (Figure 1a). Without MoO_2, a catalytic current was only observed starting from -2.5 V vs. Fe/Fc^+ and the current was much smaller (Figure 1a). The electrocatalytic activity of MoO_2 is even higher at -20°C (Figure 1b). The catalytic current was already observed at -1.6 V vs. Fe/Fc^+. At a same potential, the current is much higher at -20°C than at RT (compare Figure 1a and 1b). The temperature-dependence of activity is probably partially due to the difference in CO_2 solubility, although more study is required to elucidate its origin. It was previously reported that in MeOH + KOH electrolyte, the reduction of CO_2 by Au was more selective at low temperatures than at RT due to the suppression of hydrogen evolution at low temperatures.[20] However, in that system, the

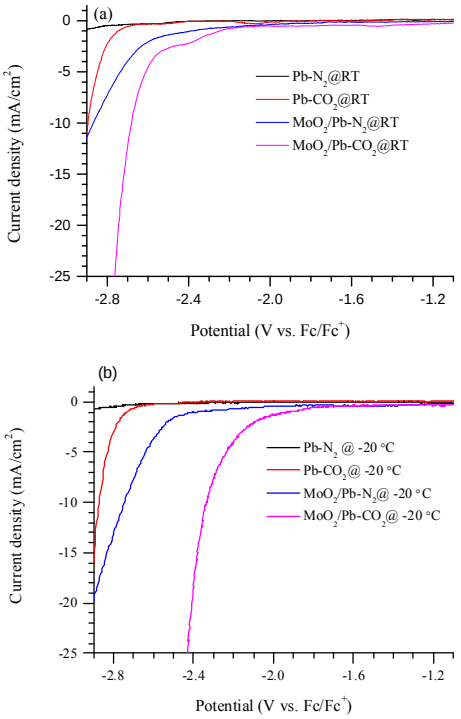

Fig. 1 Polarization curves of the MoO_2/Pb and Pb electrodes. (a) Data measured at room temperature; (b) Data measured at -20 °C. Electrolyte: 0.1 M $TBAPF_6$; scan rate: 50 mV/s.

partial current density for CO_2 reduction still decreased at low temperatures, which is opposite to what is observed in the current system.

Figure S4, ESI shows the time-dependent current response of potentiostatic electrolysis measurements of a MoO_2-modified Pb electrode at -2.45 V vs. Fe/Fc^+ in a CO_2-satureated MeCN solution. At RT, the current stayed at about -4 mA/cm^2 during 30 min; at -20^{o}C, the current was about -23 mA/cm^2. The higher current observed at -20^{o}C is consistent with the results from voltammetry measurements in Figure 1. It is noted that the background current (under N_2) was higher at RT than at -20^{o}C (Figure S5, ESI), presumably due to the suppression of hydrogen evolution at low temperatures. To further probe the long-term catalytic stability of the MoO_2/Pb electrode, an electrolysis was conducted during 5 h at -2.45 V vs. Fc/Fc^+ at -20 °C (Figure S6 (a), ESI). The current density remained at -20 mA/cm^2 during the electrolysis, indicating a good stability. Additionally, a galvanostatic electrolysis at -8.3 mA/cm^2 was conducted during 3 h; the electrode potential remained at -2.4 V vs. Fe/Fc^+ (Figure S6(b), ESI), again indicating a good catalytic stability.

During electrolysis at -20^{o}C, gas evolution around the electrode was visible. Analysis of the headspace of the electrolysis cell by gas chromatography confirmed the formation of CO. The liquid phase was analysed by ion chromatography (IC) to detect oxalate and formate (Tables S1 and S2, ESI). These products (CO, oxalate, formate) were not detected when the electrolysis was conducted in N_2-saturated solution (Figure S5 and Table S3, ESI), confirming that they originated from catalytic CO_2 reduction.

The electrolysis was conducted at three different potentials. Figure 2 shows that the potential-dependent Faradaic efficiency (FE) for the three CO_2 reduction products (CO, formate, oxalate). At RT, no CO was formed, but both formate and oxalate were produced. The maximum FE of about 40% of formate was obtained at -2.45 V; the maximum FE of about 45% of oxalate was obtained at -2.60 V. At -20 °C, CO was produced, with a FE of about 30% at -2.45 V and -2.6 V. Oxalate was also produced, with a FE of about 45% at -2.45 V and -2.6 V. At both temperatures, H_2 formation was negligible.

The mechanism of CO_2 reduction in an organic solvent such as DMF and MeCN was proposed as sequence of eqs (1)-(9).[6, 21] CO, oxalate, and formate are all possible products.

$$CO_2 + e^- \rightarrow CO_2^{\bullet-} \quad (1)$$

$$2\ CO_2^{\bullet-} \rightarrow \quad (2)$$

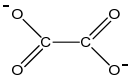

$$CO_2^{\bullet-} + H^+ + e^- \rightarrow CO + OH^- \quad (3)$$

$$CO_2^{\bullet-} + CO_2 \rightarrow \quad (4)$$

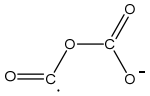

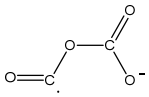

$$+ e^- \rightarrow CO + CO_3^{2-} \quad (5)$$

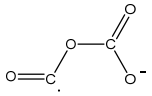

$$+ CO_2^{\bullet-} \rightarrow CO + CO_3^{2-} + CO_2 \quad (6)$$

$$CO_2^{\bullet-} + H_2O \rightarrow HCO_2^{\bullet} + OH^- \quad (7)$$

$$HCO_2^{\bullet} + e^- \rightarrow HCO_2^- \quad (8)$$

$$HCO_2^{\bullet} + CO_2^{\bullet-} \rightarrow HCO_2^- + CO_2 \quad (9)$$

CO might be produced via two different pathways: one involves the protonation of $CO_2\bullet$- by trace water or the solvent (eq. 3), while the other involves the reaction of $CO_2\bullet$- with CO_2 to give CO and carbonate (eq. 6). Formate, on the other hand, can only be produced with a proton source (eqs 7-8). It follows that water content of the solvent will have an important influence in the product formation. This influence was then investigated by addition of a known amount of water to the electrolyte solution. At RT, addition of even a small amount of water (0.1 M) led to predominant formation of H_2 (Figure S7 and Table S2, ESI). At -20 °C, however, water promotes MoO_2-catalyzed CO_2 reduction.

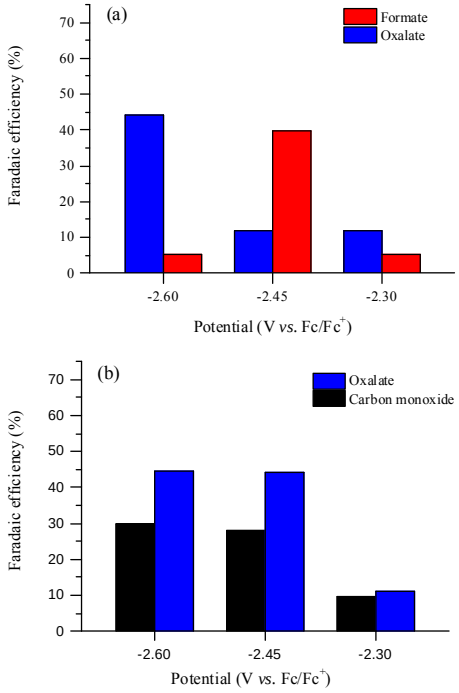

Fig. 2 Potential-dependent Faradaic yields of the formation of CO, formate, and oxalate from catalytic CO_2 reduction. (a) Data were obtained at room temperature; (b) data were obtained at -20 °C.

Figure 3 shows the polarization curves for CO_2 reduction were shifted to more positive potentials when incremental amounts of water were added to the electrolyte solution. At 1.4 M water concentration, catalytic current was observed at as low as -1.5 V vs. Fe/Fc^+. The influence of water content in the product distribution of MoO_2-catalyzed CO_2 reduction at -2.45 V vs. Fe/Fc^+ at -20^{o}C is depicted in Figure 4. The FE of CO increased initially with an increase in water concentration, reaching a maximum of about 70% with 0.4 M water. Further increase of water concentration then diminished the FE of CO formation. The FE of formate, on the other hand, increased continuously with an

increase in water concentration. At a low water concentration, only a small amount of formate was produced; at 1.4 M water concentration, the FE of formate reached 55%. As water promoted the formation of CO and formate, the FE of oxalate decreased as more water was present. Even though water should be beneficial for hydrogen evolution and indeed some H_2 was produced upon addition of water, the FE of H_2 did not exceed 20% even at 1.4 M water concentration. Overall, the data in Figure 4 suggests that when water is present, formation of CO and formate is competing against one another. At a low water concentration, eq. 3 is favoured and CO is the main product. At a high water concentration, eq. 7 is favoured and formate is the main product.

It was earlier reported that Mo metal was active for CO_2 reduction in water.[22] The CO_2 reduction by the MoO_2/Pb electrode operates in MeCN and gives a different production distribution than Mo-catalyzed CO_2 reduction in water. However, it is possible that MoO_2 is reduced to Mo metal nanoparticles during electrolysis, and the in-situ formed Mo nanoparticles are the catalytically active species. Several experiments were conducted to test this possibility. First, the MoO_2/Pb electrode was subjected to CO_2 reduction for 3 h and then characterized by XRD. Figure S8, ESI shows that diffraction patterns corresponding to MoO_2 remained after electrolysis, and no significant peaks corresponding to Mo was observed. Second, a Mo metal rod electrode was tested for CO_2 reduction under the same conditions. However, no significant catalytic current was observed either in polarization measurements (Figure S9, ESI) or in potentiostatic electrolysis at -2.6 V vs. Fe/Fc^+ (Figure S10, ESI). These results largely rule out the possibility that in-situ produced Mo metal acts as the catalytically active species.

After confirming the role of MoO_2 in the catalysis, we probed the role of the electrolyte. This was motivated by earlier reports that organic molecules could serve as co-catalysts and mediators for CO_2 reduction.[4] For example, Bockris and Wass showed that tetraalkylammonium cations could mediate one-electron reduction of CO_2 by forming radical intermediates.[23] We found a similar activity for the reduction of CO_2 when the $TBAPF_6$ electrolyte was replaced by $TBAClO_4$ (Figure S11(a) and Table S5, ESI). On the other hand, no significant CO_2 reduction activity was observed when the $TBAPF_6$ electrolyte was replaced by $LiClO_4$ (Figure S11(b) and Table S5, ESI). These results indicate an important role of TBA cations in the catalysis. We propose that TBA^+ act as a one-electron mediator to promote the reduction of CO_2 by MoO_2.

The overpotential of the current system is also evaluated. Savéant and co-workers calculated the thermodynamic potential of CO_2 reduction to CO to be at -0.89 V vs. saturated calomel electrode (SCE) in MeCN, which is equivalent to -1.29 V vs. Fe/Fc^+.[24, 25] According to Figure 3, a significant current was observed at -1.5 V vs. Fe/Fc^+. This suggests that CO_2 reduction occurs already at an overpotential of below 200 mV which indicates a very active CO_2 reduction catalyst. Certainly a much larger overpotential is required to reach a practically meaningful current density (e.g., 5-10 mA/cm^2); however, the net overpotential at high currents includes significant contributions from the high resistance of the MeCN solution and the mass transport of CO_2.

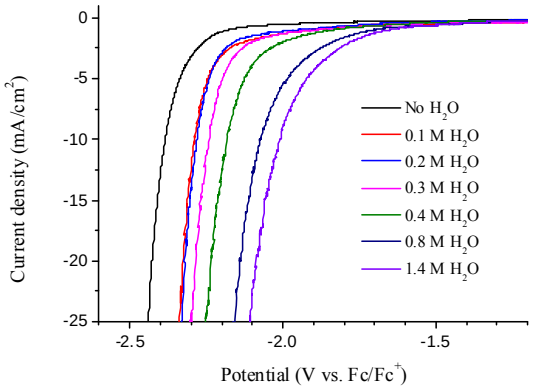

Fig. 3 Influence of water concentration in the polarization curves of MoO_2/Pb in CO_2-saturated MeCN at -20 °C. Electrolyte: 0.1 M $TBAPF_6$; scan rate: 50 mV/s.

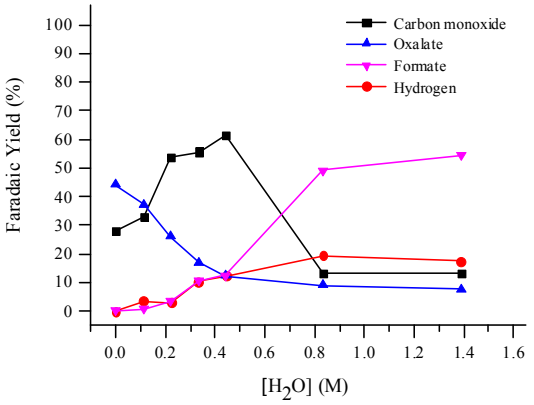

Fig. 4 Faradaic yield of CO_2 reduction as a function of water content. Potentiostatic electrolysis was carried at -2.45 V vs. Fc/Fc^+ at -20 °C in 0.1 M $TBAPF_6$/MeCN.

The activity of MoO_2 towards CO_2 reduction was then studied in DMF. Figure S12, ESI shows that catalytic waves for CO_2 reduction were observed at both RT and -20 °C. Again the activity is higher at -20°C. The onset potentials were about 2.0 V vs. Fc/Fc^+ at both temperatures. Electrolysis was conducted in DMF as well (Table S4, ESI). CO, formate, and oxalate were produced at both RT and -20 °C. At RT and -2.45 V, the major product was CO (50%) and formate (41%); at -20 °C at -2.45 V, the major product was also CO (40%) and formate (41%). When water was added, a significant amount of H_2 was produced at both temperatures. MoO_2 was also tried for CO_2 reduction in water. However, hydrogen evolution was the main reaction.

In conclusion, the catalytic activity of MoO_2, a readily available metal oxide, for electrochemical CO_2 reduction is reported for the first time. The onset overpotential for CO_2 reduction in MeCN is below 200 mV. The activity is much higher at -20 °C than at RT, and this activity is promoted by a small amount of water. The selectivity of CO_2 reduction depends on temperature and water content. At -20 °C, water favors the formation of CO and formate over oxalate. Conditions for a FE of 70% for CO formation or a FE of 55% for formate formation have been identified.

This work is supported by a European Research Council starting grant (no. 257096).

Notes and references

Laboratory of Inorganic Synthesis and Catalysis, Institute of Chemical Sciences and Engineering, Ecole Polytechnique Fédérale de Lausanne (EPFL), EPFL-ISIC-LSCI, BCH 3305, Lausanne, CH 1015, Switzerland. Fax: 41 216939305; Tel: 41 216939781; E-mail: xile.hu@epfl.ch†
Electronic Supplementary Information (ESI) available: experimental details, additional figures and tables. See DOI: 10.1039/b000000x/

1. A. M. Appel, J. E. Bercaw, A. B. Bocarsly, H. Dobbek, D. L. DuBois, M. Dupuis, J. G. Ferry, E. Fujita, R. Hille, P. J. A. Kenis, C. A. Kerfeld, R. H. Morris, C. H. F. Peden, A. R. Portis, S. W. Ragsdale, T. B. Rauchfuss, J. N. H. Reek, L. C. Seefeldt, R. K. Thauer and G. L. Waldrop, *Chem. Rev.*, 2013, **113**, 6621-6658.
2. Y. Hori, in *Modern Aspects of Electrochemistry*, eds. C. G. Vayenas, R. E. White and M. E. Gamboa-Aldeco, Springer, New York, 2008, vol. 42, pp. 89-189.
3. E. E. Benson, C. P. Kubiak, A. J. Sathrum and J. M. Smieja, *Chem. Soc. Rev.*, 2009, **38**, 89-99.
4. Y. Oh and X. L. Hu, *Chem. Soc. Rev.*, 2013, **42**, 2253-2261.
5. Y. Hori, H. Wakebe, T. Tsukamoto and O. Koga, *Electrochim. Acta* 1994, **39**, 1833-1839.
6. A. Gennaro, A. A. Isse, M. G. Severin, E. Vianello, I. Bhugun and J. M. Saveant, *J. Chem. Soc.- Faraday Trans.*, 1996, **92**, 3963-3968.
7. M. Gattrell, N. Gupta and A. Co, *J. Electroanal. Chem.*, 2006, **594**, 1-19.
8. W. Tang, A. A. Peterson, A. S. Varela, Z. P. Jovanov, L. Bech, W. J. Durand, S. Dahl, J. K. Norskov and I. Chorkendorff, *Phys. Chem. Chem. Phys.*, 2012, **14**, 76-81.
9. C. W. Li and M. W. Kanan, *J. Am. Chem. Soc.*, 2012, **134**, 7231-7234.
10. K. J. P. Schouten, Y. Kwon, C. J. M. van der Ham, Z. Qin and M. T. M. Koper, *Chem. Sci.*, 2011, **2**, 1902-1909.
11. K. P. Kuhl, E. R. Cave, D. N. Abram and T. F. Jaramillo, *Energy Environ. Sci.*, 2012, **5**, 7050-7059.
12. Y. H. Chen, C. W. Li and M. W. Kanan, *J. Am. Chem. Soc.*, 2012, **134**, 19969-19972.
13. B. A. Rosen, A. Salehi-Khojin, M. R. Thorson, W. Zhu, D. T. Whipple, P. J. A. Kenis and R. I. Masel, *Science*, 2011, **334**, 643-644.
14. J. L. DiMeglio and J. Rosenthal, *J. Am. Chem. Soc.*, 2013, **135**, 8798-8801.
15. Y. H. Chen and M. W. Kanan, *J. Am. Chem. Soc.*, 2012, **134**, 1986-1989.
16. H. Vrubel, D. Merki and X. L. Hu, *Energy Environ. Sci.*, 2012, **5**, 6136-6144.
17. D. Merki, H. Vrubel, L. Rovelli, S. Fierro and X. L. Hu, *Chem. Sci.*, 2012, **3**, 2515-2525.
18. H. Vrubel and X. L. Hu, *Angew. Chem., Int. Ed.*, 2012, **51**, 12703-12706.
19. Y. Tomita, S. Teruya, O. Koga and Y. Hori, *J Electrochem Soc*, 2000, **147**, 4164-4167.
20. S. Kaneco, K. Iiba, K. Ohta, T. Mizuno and A. Saji, *J. Electroanal. Chem.*, 1998, **441**, 215-220.
21. C. Amatore and J. M. Saveant, *J. Am. Chem. Soc.*, 1981, **103**, 5021-5023.
22. D. P. Summers, S. Leach and K. W. Frese, *J. Electroanal. Chem.*, 1986, **205**, 219-232.
23. J. O. Bockris and J. C. Wass, *J. Electrochem. Soc.*, 1989, **136**, 2521-2528.
24. C. Costentin, S. Drouet, M. Robert and J. M. Saveant, *Science*, 2012, **338**, 90-94.
25. N. G. Connelly and W. E. Geiger, *Chem. Rev.*, 1996, **96**, 877-910.